

### F-center stabilization process in the first coloring stage of alkali halide crystals

E. R. Hodgson, A. Delgado, and J. L. Alvarez Rivas

Junta de Energía Nuclear, Madrid 3, Spain

(Received 26 January 1978)

Detailed measurements of the first-stage *F*-coloring and *F*-thermal-annealing curves between 15 and 65°C indicate a clear correlation between the structure of the *F*-coloring curve, the *F*-thermal-annealing steps, and the thermoluminescence. A model based on interstitial trapping gives a concise physical picture for these processes and permits a unified treatment for the phenomena, which clarifies the complex problem of the temperature and dose-rate dependence in *F*-coloring curves.

#### I. INTRODUCTION

Over the years, studies have been made of the first-stage *F* coloration of alkali-halide crystals, as may be seen in the comprehensive review by Sonder and Sibley,<sup>1</sup> in which the most important references are given.<sup>2-5</sup> From the beginning, attempts were made to fit mathematically the coloring curves. However a coherent model was lacking, particularly as to the experimental justification of the fitting parameters.

It is known that there is interstitial creation and trapping even in the first-stage *F*-coloring process.<sup>1</sup> A simple model based on interstitial trapping has been presented<sup>6</sup> in which a various component exponentially saturating growth of the coloring curve is predicted, with the fitting parameters representing physically meaningful entities. It has

been proposed that the *F*-center thermal annealing and the thermoluminescence (TL) in irradiated pure alkali halides is due to *F*-center-interstitial recombination.<sup>7</sup> Hence, it is reasonable to search for a correlation between these three processes, (the coloring curve, the *F* annealing, and TL) and in this way demonstrate the validity of the model.

#### II. EXPERIMENTAL METHOD

The same in-beam method used in the earlier work<sup>6</sup> has been employed, the spectrophotometer being modified to permit the measurement of optical absorption at two distinct wavelengths (in this case the *F* and *M* centers) and measurement of the luminescence emitted by the sample during irradiation, Fig. 1.

A pure NaCl sample, cleaved from a single

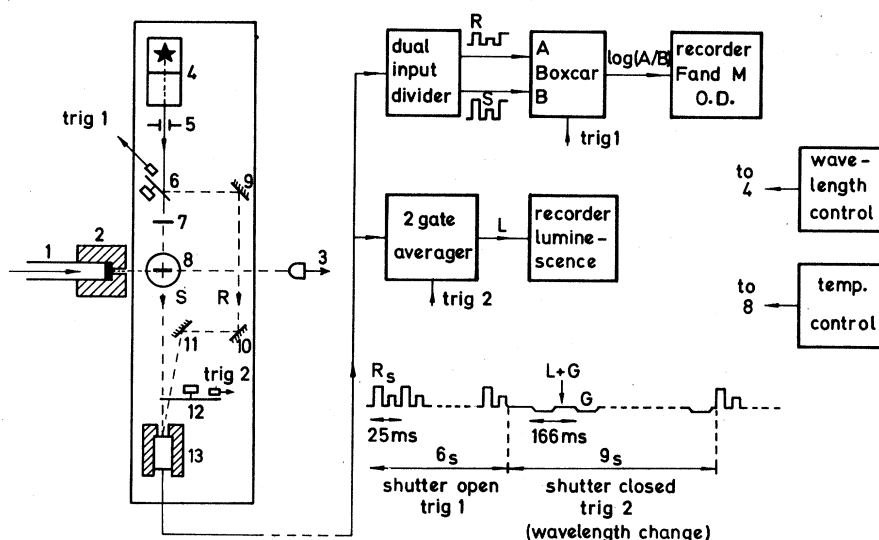


FIG. 1. Experimental setup. (1) 1.8-MeV electrons stopped in a water-cooled gold target; (2) lead collimator; (3) ionization chamber, for dose rate control; (4) lamp and double grating monochromator (Bausch and Lomb); (5) shutter; (6) fast chopper; (7) neutral filter; (8) evacuated sample chamber with heating oven; (9), (10), and (11) mirrors; (12) luminescence chopper; (13) photomultiplier with lead shield; (R) reference pulse; (S) signal pulse.

Harshaw crystal block, was irradiated in an evacuated chamber with bremsstrahlung  $\gamma$  rays, producing a constant dose rate at the sample of  $1.3 \times 10^4$  R/h. The  $F$ - and  $M$ -center sample colorings were measured simultaneously together with the luminescence emitted. At the end of the irradiation period the sample was heated *in situ* to  $350^\circ\text{C}$  and the consequent  $F$  and  $M$  thermal annealing, and the TL, were recorded. At the end of each measurement the sample was allowed to cool slowly to  $15^\circ\text{C}$  ready for the next irradiation. No aging effects have been observed during the whole experimental period. The measurements have been performed for sample temperatures between  $15$  and  $95^\circ\text{C}$  in steps of  $10^\circ\text{C}$ , each sample temperature being maintained constant to within  $0.5^\circ\text{C}$  during the irradiation periods.

The sequence used during irradiation and thermal annealing was to measure the  $F$ -center absorption for 6 sec. Then to change the monochromator wavelength, during which time the shutter cuts off the monochromator light permitting the sample luminescence to be measured for a period of about 9 sec. This is followed by an  $M$  center absorption measurement and then a further luminescence measurement during a monochromator change to the  $F$ -center wavelength. This sequence is repeated automatically during the whole experiment.

The fast chopper divides the monochromator light beam producing a pulsed signal beam  $S$  which passes through the sample and a pulsed reference beam  $R$ . The signal and reference give a series of pulses at the photomultiplier output which are fed to a dual input divider and then to a two-channel boxcar signal averager (PAR model 162). The reference pulse entering input gate  $A$  and the signal pulse entering gate  $B$  are adjusted for equal amplitude by means of the input divider at the beginning of each experiment. In this way, the analogue boxcar output,  $\log_{10}(A/B)$  starts from zero permitting null sensitivity, and is directly proportional to the optical density of the sample. Trigger 1 from the fast chopper is used to synchronize the gates  $A$  and  $B$  with the reference and signal pulses. A set of neutral filters is used to reduce the signal beam intensity, hence minimizing bleaching. However the  $\gamma$  background at the photomultiplier imposes a lower limit on the signal beam intensity due to the decreasing signal-to-noise ratio. Despite the compromise, the effects of bleaching and background have been reduced to negligible levels.

The luminescence chopper during the  $F$  and  $M$  optical-density measurements is stopped in a position permitting the signal and reference beams to enter the photomultiplier. Immediately after an  $F$  or  $M$  measurement, the luminescence chopper

starts, thus modulating the sample luminescence. This modulation is necessary due to the fact that the sample luminescence ( $L$ ) received by the photomultiplier is small compared with the  $\gamma$ -radiation background ( $G$ ). The modulated signal is fed into a two gate signal averager which gives an output proportional to the modulation amplitude  $L$ . Trigger 2 from the luminescence chopper synchronizes the two gates with  $L+G$  and  $G$ .

All the data output is fed to paper chart recorders and the optical-density information is also punched onto paper tape for computer analysis.

### III. RESULTS

Below  $60^\circ\text{C}$  the  $M$ -center formation is low compared with the  $F$ -center formation (about 3%), and does not affect the  $F$ -center production. However above this temperature the  $M$ -center production rate rapidly increases, markedly affecting the  $F$ -center concentration to such an extent as to pro-

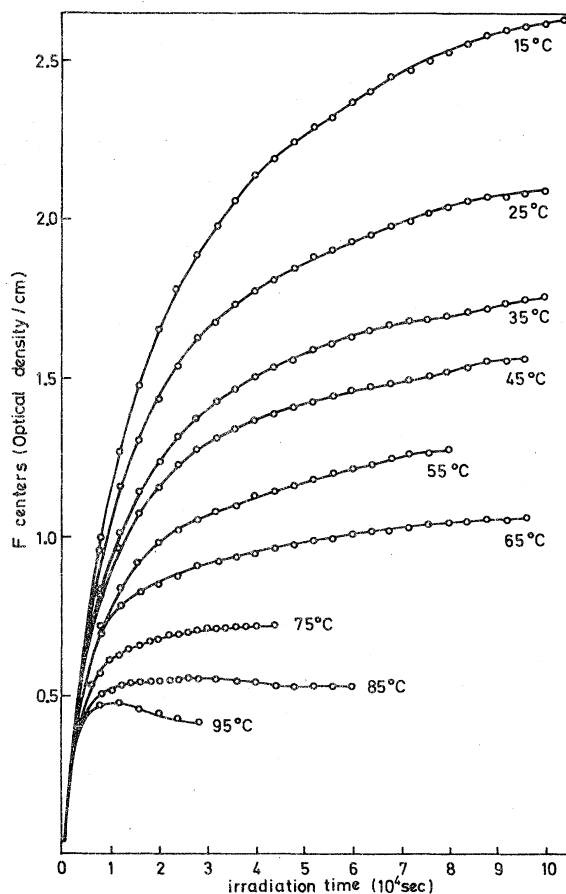


FIG. 2.  $F$ -coloring curves for a pure NaCl Harshaw sample ( $15 \times 15 \times 4$  mm) irradiated at a dose rate of  $1.3 \times 10^4$  R/h.

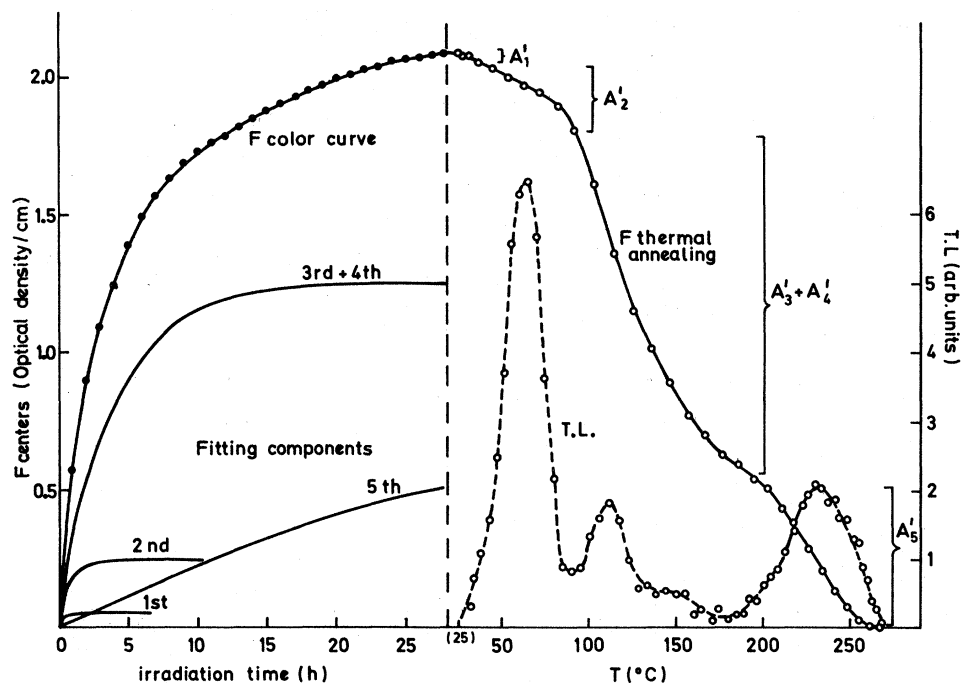


FIG. 3. 25°C results showing the  $F$ -coloring curve, the  $F$  thermal annealing, TL, and the fitting components. The fitting partial amplitudes  $A'_i$  are indicated next to the corresponding  $F$  annealing steps.

duce a maximum in the  $F$ -coloring curve. This supports our earlier suggestion, that  $M$ -center production is responsible for the observed maxima. Due to this phenomenon, the high-temperature data will be presented in a subsequent paper to include the  $M$ -center production and sample luminescence during irradiation. Here we only discuss the  $F$ -center results for 15–65°C.

Figure 2 shows all the  $F$ -color curves (15–95°C) obtained during irradiation and Fig. 3 shows the 25°C  $F$  curve together with the corresponding  $F$  thermal annealing and TL curves. The coloring curves have been fitted by exponentially saturating components using a computer program. The equation for the optical density  $F_{OD}$  is

$$F_{OD} = \sum_{i=1}^n A_i (1 - e^{-a_i t}),$$

$A_i$  and  $a_i$  being the variable parameters. In the earlier work,<sup>6</sup> we used a fitting equation in which a linear term  $a_i t$  was included to account for any possible first stage trap creation. However from these more detailed measurements, we find no evidence for a linear term, the slow almost linear growth being accounted for by a long-lifetime component. The number of components used in the fitting is the minimum necessary so that the addition of a further component does not significantly reduce the  $\chi^2$  value for the fit. In this way the color

curves have been fitted by up to four components. The experimental and fitting methods impose limits beyond which the  $1/a$  values are not reliable. An upper limit of approximately  $5 \times 10^4$  sec is due to the maximum irradiation time used (irradiation times longer than about 30 h were not feasible due to various technical problems beyond our control). The lower limit for  $1/a$  is about 600 sec due to the fact that the  $F$  optical density is only measured every 30 sec and the fitting program requires about 20 points for an appreciable  $\chi^2$  variation. The overall errors for the  $A_i$  and  $a_i$ , taking into account both experimental and fitting procedures, are approximately 20%, as indicated in Fig. 4.

In Fig. 3 the fitting components for the 25°C curve are shown. The first component ( $i=1$ ), has been observed at 15 and 25°C, and also at 15 and 20°C for color curves obtained at double the dose rate ( $2.8 \times 10^4$  R/h). The corresponding  $F$  thermal annealing curve shows three main steps, however the second step (90–180°C) is a superposition of at least two unresolved steps as may be clearly seen by obtaining the spectrum derived from the  $F$  annealing curve. Annealing curves obtained after irradiation at 15°C indicate that the first main step is preceded by an initial small step. In the figure, one can observe the good agreement between the  $F$  annealing step amplitudes and the values  $A'_i$ , where  $A'_i = A_i (1 - e^{-a_i t})$  for  $t$  equal to the

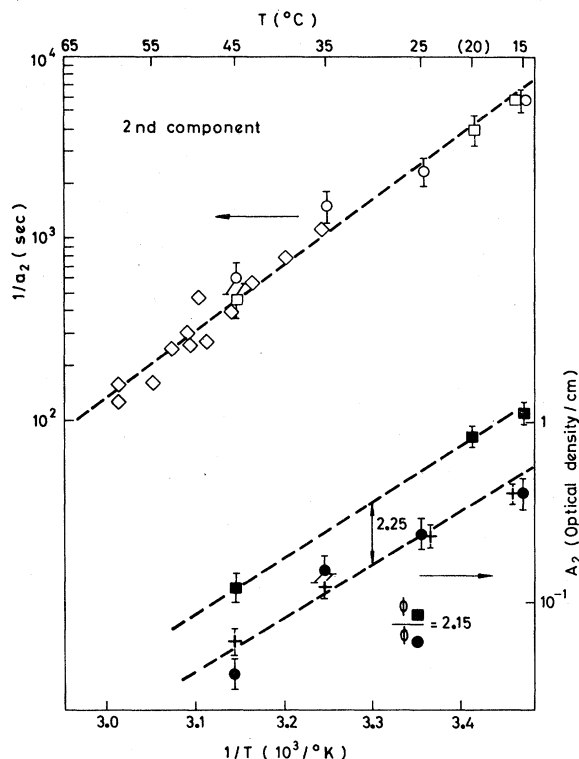


FIG. 4. Temperature dependence of  $A_2$  and  $1/a_2$  together with annealing step and TL comparisons, and effect of doubling the dose rate.  $\bullet A_2$ ,  $\circ 1/a_2$ ,  $\blacktriangle$  annealing step,  $\diamond$  TL data for 60°C glow peak,  $\blacksquare A_2$ , and  $\square 1/a_2$  at double the dose rate.

total irradiation time. Clearly for components which saturate during the irradiation time,  $A'_i = A_i$ .

Figure 4 shows the temperature dependence of the fitting parameter  $A_2$  and also the correlation between the second step amplitude and  $A_2$ . In Fig. 5(a),  $A'_5 = A_5(1 - e^{-a_5 t})$  for  $t$  equal to the total irradiation time, as this component does not reach saturation, is shown as a function of temperature together with the correlation between  $A'_5$  and the fifth step amplitude. In Fig. 5(b) the results for the first component  $A_1$  are shown. The corresponding  $F$  annealing step amplitudes are also given.

In Fig. 6, the results for the third and fourth components are shown. Between 15 and 35°C these components are not resolved in the fitting and the resulting component is given as  $i=3$ . However at 45 and 55°C the two are resolved and shown as  $i=3$  and  $i=4$ . By 65°C the third component is too small to be measured. In the case of the  $F$  annealing one clearly sees a third and fourth step, however their separate amplitudes are difficult to determine. In the figure the total amplitude for these two steps is shown. These total step am-

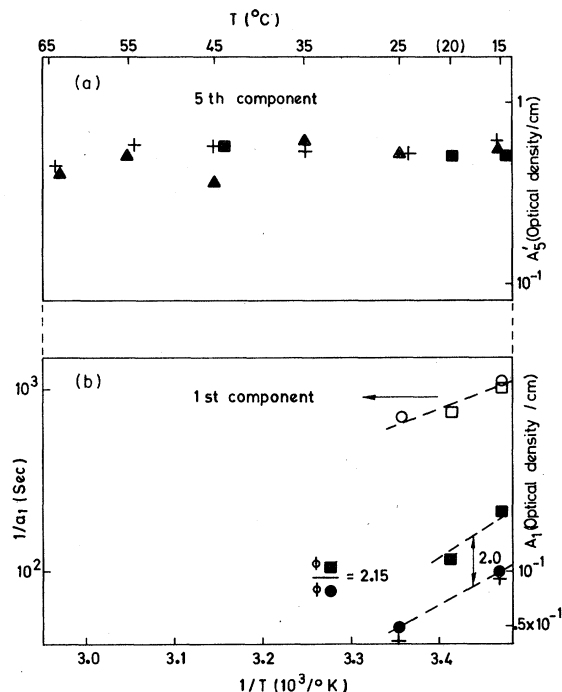


FIG. 5. (a) Temperature dependence of  $A'_5$  with annealing step comparison and effect of doubling the dose rate.  $\blacktriangle A'_5$ ,  $\blacktriangle$  annealing step,  $\blacksquare A'_5$  at double the dose rate for the same total dose. (b) First component results.  $\bullet A_1$ ,  $\circ 1/a_1$ ,  $\blacktriangle$  annealing step,  $\blacksquare A_1$ , and  $\square 1/a_1$  at double the dose rate.

plitudes agree well with the predominant fitting component amplitude, the third below 35°C and the fourth above 35°C.

We now present the results for the fitting parameters  $a_i$ . In Figs. 4, 5(b), and 6 the parameters  $1/a_1$ ,  $1/a_2$ ,  $1/a_3$ , and  $1/a_4$  are shown. The  $1/a_5$  are not shown as these values are included in the  $A'_5$ , this being the only reliable entity for this long lifetime component. The resolution considerations discussed earlier for the third and fourth component amplitudes  $A_3$  and  $A_4$ , apply equally to the fitting components  $a_3$  and  $a_4$ .

As can be seen in Fig. 3, there is a clear temperature correlation between the  $F$ -center annealing steps and the glow peaks of the TL spectrum which have been simultaneously measured. This correlation is in agreement with earlier measurements.<sup>7</sup> The lifetimes of the TL processes measured by Mariani *et al.*<sup>8</sup> are also given in Figs. 4 and 6. The use of this data is justified by the fact that the samples used were cleaved from the same Harshaw block, and that the  $F$ -center concentrations were of the same order. It can be seen that the extrapolated lifetimes for the 60°C glow peak are in excellent agreement with the fitted lifetimes

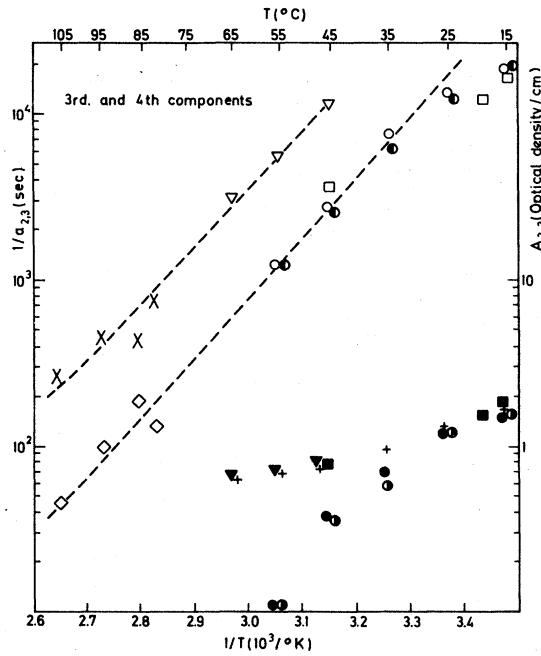


FIG. 6. Results for the third and fourth components. ●  $A_3$ , ○  $1/a_3$ , + annealing step, ◇ TL data for the 110°C glow peak, ■  $A_3$ , and □  $1/a_3$  at double the dose rate, ○  $A_3$  and ●  $1/a_3$  intermediate case predictions, ▽  $A_4$ , ▽  $1/a_4$ , × TL data for the 150°C glow peak.

for the second exponential component, Fig. 4. No TL data is available for comparison with the first component. In the case of the fifth component, the extrapolated TL data indicates lifetime values  $\gg 10^5$  sec. The correlation between the third and fourth component  $1/a$  values and the TL lifetime data for the 110 and 150°C glow peaks is shown in Fig. 6. Although in this case there is no overlap in the temperature range for the measurements, the agreement between the two sets of data is good.

#### IV. DISCUSSION

The correlations between the fitting parameters  $A_i$  and  $1/a_i$ , and the annealing step amplitudes and the glow peak lifetimes, respectively, indicate that the fitting procedure used is not purely mathematical, but that each exponentially saturating growth component corresponds to a real physical process. More important however, is the obvious conclusion that the  $F$ -center coloring process, the  $F$ -center thermal annealing process and associated TL are closely related phenomena which should allow a unified treatment.

A simple model based on interstitial trapping already published,<sup>6</sup> predicts a various component exponentially saturating growth for the coloring curve due to the filling of distinct types of traps, and leads to the following expressions for the fitting parameters

$$A_i = (\sigma_i \phi N_{0i}) / (\sigma_i \phi + 1/\tau_i), \quad a_i = \sigma_i \phi + 1/\tau_i,$$

where  $N_{0i}$  is the concentration of traps of type  $i$ ,  $\sigma_i$  is the trap cross section,  $\tau_i$  the lifetime of an interstitial in trap  $i$ , and  $\phi$  the flux of interstitials during irradiation, assumed to be constant and directly proportional to the dose rate.

The reverse process in which the interstitials are liberated from these traps to recombine with  $F$  centers, leads to the  $F$ -center thermal annealing and associated TL phenomena. Hence the lifetime  $\tau_i$  in the model is that corresponding to the glow peak of trap  $i$ , and the  $A_i$  the thermal annealing step amplitudes. The temperature dependence of  $\tau_i$  is  $\tau_i = \tau_{0i} \exp(E_i/kT)$ . This is expected to be the only temperature-dependent term in the two fitting parameters. Evidence that this is so is given in Table I, where the products  $A_i a_i = \sigma_i \phi N_{0i}$  are listed. These products show little or no temperature dependence. Furthermore, as  $N_{0i}$  is a constant for a particular type of trap, one may con-

TABLE I. Products  $A_i a_i = \sigma_i \phi N_{0i}$ .

$T$ (°C)	$A_i a_i (10^{-4} \text{ OD/cm sec})$				
	$A_1 a_1$	$A_2 a_2$	$A_3 a_3$	$A_4 a_4$	$A_5 a_5$
15	0.90 ± 0.20	0.86 ± 0.20	0.83 ± 0.20	...	0.078 ± 0.020
25	0.74 ± 0.25	1.04 ± 0.25	0.92 ± 0.25	...	0.077 ± 0.020
35	...	1.00 ± 0.25	0.93 ± 0.25	...	0.137 ± 0.030
45	...	0.70 ± 0.30	1.29 ± 0.30	0.69 ± 0.30	0.039 ± 0.010
55	...	...	0.89 ± 0.25	1.30 ± 0.30	0.115 ± 0.025
65	...	...	...	2.20 ± 0.50	0.111 ± 0.025

clude that  $\sigma_i\phi$  is temperature independent. The exception in the case  $A_4a_4$  is most probably due to resolution problems.

We now consider the model predictions for three specific cases.

#### A. Condition $\sigma_i\phi$ small compared with $1/\tau_i$

The fitting parameters reduce to  $A_i = \sigma_i\phi N_{0i}\tau_i$ ,  $1/a_i = \tau_i$ . In this case the  $1/a_i$  values are the same as the TL lifetimes, which is clearly observed for component  $i=2$ , Fig. 4. As the product  $\sigma_2\phi N_{02}$  is temperature independent (see Table I), the two parameters  $A_2$  and  $1/a_2$  should have the same exponential temperature dependence. This is observed to be the case. Furthermore, the parameter  $1/a_i$  is dose rate independent, while the parameter  $A_i$  is directly proportional to dose rate. Data obtained at double the dose rate is included in Fig. 4 for component  $i=2$  and is in excellent agreement with these predictions. The few results obtained for component  $i=1$ , Fig. 5(b), indicate that this component is also included in the case  $\sigma_i\phi$  small compared with  $1/\tau_i$ . No TL data is available for comparison.

#### B. Condition $\sigma_i\phi$ large compared with $1/\tau_i$

Here the fitting parameters reduce to  $A_i = N_{0i}$  and  $a_i = \sigma_i\phi$ . Thus  $A_i$  is temperature independent and  $a_i$  has the same temperature dependence as  $\sigma_i\phi$ .

In the case of component  $i=5$ , the fitting procedure yields ill-defined values for the individual  $A_5$  and  $a_5$  due to the long lifetime of this component. (An estimated 300 h of irradiation would be necessary to determine the individual  $A_5$  and  $a_5$  values.) Despite this problem the products  $A_5a_5$  show no clear temperature dependence, see Table I. It is observed for components  $i=1, 2, 3$  that  $A_ia_i$  is not temperature dependent. It seems reasonable therefore to assume that  $A_5a_5$  is also temperature independent. With this assumption, the partial amplitude  $A_5' = N_{05}(1 - e^{-\sigma_5\phi t})$  which is well determined in the fitting, should be temperature independent. This is clearly observed to be so, see Fig. 5(a).

In this second limiting case,  $A_i$  is dose rate independent, while  $a_i$  is directly proportional to the dose rate. This results in the partial amplitude  $A_5'$  being dose rate independent as  $\phi$  occurs as a product  $\phi t$ . Data for the fifth component obtained at double the dose rate is shown in Fig. 5(a) for

the same dose and is in good agreement with the prediction.

#### C. Condition $\sigma_i\phi$ and $1/\tau_i$ of the same order

This condition will only apply within a very limited temperature range as  $\tau_i$  varies exponentially with temperature and one rapidly passes to conditions *A* or *B* on increasing or decreasing the temperature respectively. Both fitting parameters  $A_i$  and  $1/a_i$  should show the same temperature dependence, assuming little dependence in  $\sigma_i\phi$ . The parameters are both dose rate dependent in this range, with  $A_i$  increasing and  $1/a_i$  decreasing with dose rate.

From the results obtained, the third component is consistent with such an intermediate transitional case, see Fig. 6. The model predictions for this case are also shown in the figure, normalized to the data with  $\sigma_3\phi \approx 1/\tau_3$  at 15°C changing to  $\sigma_3\phi$  small compared with  $1/\tau_3$  by 45°C. Data obtained at double the dose rate are also given in Fig. 6 and are consistent with the expected dose rate dependence. The fourth component is not well enough determined to use the data below 55°C.

It is interesting to note that the products  $A_ia_i$  ( $i=1, 2, 3$ ) are equal, within the experimental errors. It is unlikely that this is fortuitous, and may indicate that a single crystal defect can induce several distinct interstitial traps. However, one requires much more data to speculate over this point.

## V. CONCLUSIONS

All the results indicate that the *F*-center coloring process, the *F*-center thermal annealing process and associated thermoluminescence are closely related phenomena which allow a unified treatment based on a simple interstitial trapping model.

It is clear from the model that the interpretation of experiments on the dose rate dependence of the first stage in the *F*-coloring curves is not straightforward. One must bear in mind the  $\sigma\phi$  to  $1/\tau$  ratio which is both temperature and dose rate dependent, and moreover may be completely different for each component.

## ACKNOWLEDGMENTS

We are indebted to A. Mojado for his invaluable help both in preparing and running the experiment. We would also like to thank Dr. J. Yunta for her work in preparing the fitting program.

- <sup>1</sup>*Point Defects in Solids*, edited by J. H. Crawford and L. Slifkin (Plenum, New York, 1972), Vol. 1.
- <sup>2</sup>P. V. Mitchell, D. A. Wiegand, and R. Smoluchowski, *Phys. Rev.* **121**, 484 (1961).
- <sup>3</sup>J. L. Alvarez Rivas and P. W. Levy, *Phys. Rev.* **162**, 816 (1967).
- <sup>4</sup>P. W. Levy, P. L. Mattern, and K. Lengweiler, *Phys. Rev. Lett.* **24**, 13 (1970).
- <sup>5</sup>F. Agulló-López and F. Jaque, *J. Phys. Chem. Solids* **43**, 1949 (1973).
- <sup>6</sup>E. R. Hodgson, A. Delgado, and J. L. Alvarez Rivas, *Solid State Commun.* **16**, 785 (1975).
- <sup>7</sup>V. Ausín and J. L. Alvarez Rivas, *J. Phys. C* **5**, 82 (1972).
- <sup>8</sup>D. F. Mariani and J. L. Alvarez Rivas, *J. Phys. C* (to be published).